# A solution-phase synthesis method to highly active Pt-Co/C electrocatalysts for proton exchange membrane fuel cell

Wenzhen Li [*,1], Zhongwei Chen [2], Lianbin Xu [3], Yushan Yan [**]

*Department of Chemical and Environmental Engineering, Bourns College of Engineering, Center for Environmental Research and Technology (CE-CERT), University of California-Riverside, Riverside, CA 92521, USA*

## ABSTRACT

A solution-phase synthesis method was studied to prepare carbon supported Pt-Co alloy catalysts. The organic precursors of Pt acetylacetonate and Co acetylacetonate were reduced in a high boiling point solvent of octyl ether in the presence of oleic acid (OAc) and oleylamine (OAm) to produce fine Pt-Co nanoparticles, which were subsequently deposited on carbon support to obtain Pt-Co/C catalysts. Thermogravimetric analysis suggests that the stabilizers (OAc and OAm) can be removed by copious ethanol washing and subsequent moderate temperature heat-treatment (250 °C, under Argon atmosphere). X-ray diffraction patterns indicate that the average particle size is around 2.3 nm, and the lattice parameter is 3.868 Å for the heat-treated Pt-Co/C (40 wt%). Transmission electron microscopy images show very small Pt-Co alloy nanoparticles homogeneously dispersed on the carbon support with a particle size distribution of 2–4 nm for all Pt-Co/C samples. The elements composition of Pt and Co in the final Pt-Co/C catalyst can be well controlled, as evidenced by inductively coupled plasma atomic emission spectroscopy and energy dispersive spectroscopy analyses. Proton exchange membrane fuel cell tests show the heat-treated Pt-Co/C cathode catalyst has higher mass activity of oxygen reduction reaction than Pt/C at an operation voltage of 0.9 V, this can be attributed to its smaller particle size and reduced lattice parameter.

© 2009 Elsevier B.V. All rights reserved.

## 1. Introduction

The slow kinetic of oxygen reduction reaction (ORR) remains one of the primary challenges for wide-spread application of proton exchange membrane fuel cells (PEMFCs) [1–4]. Even at the most active noble metal catalyst Pt surface, the exchange current density of ORR at the cathode is $10^{-9}$ A cm$^{-2}$, which is six orders of magnitude lower than that of hydrogen oxidation reaction (HOR, $10^{-3}$ A cm$^{-2}$) occurred at the anode. Therefore, significant over-potential of ORR (i.e. >250 mV) exists even under the state of open circuit voltage (OCV). At a working voltage of 0.7 V, the thermal efficiency of a PEMFC is only 47%, which is much lower than the theoretical efficiency of 83% at 1.23 V [1].

It has been found that one of the most efficient ways to reduce the over-potential of ORR is to alloy a base metal M (M = Cr, Fe, Co, Ni, Cu, etc.) to form a Pt-M bimetallic catalyst, which has been confirmed to possess an enhanced ORR kinetics compared to Pt [3–24]. For example, Watanabe and co-workers found a 20-time-enhancement in ORR specific activity for a sputtered PtFe thin film catalyst over Pt [12,13]. Stamenkovic et al. further discovered that a Ni(1 1 1)@Pt single crystal prepared in ultra high vacuum (UHV) system could demonstrate 90 times improvement in ORR specific activity compared to commercial Pt/C catalyst in an *in-situ* three-electrode-cell configuration [5]. The proposed mechanisms for the ORR activity enhancement can be broadly classified as structural factors [9,10], electronic factors [11–13], inhibition by anion adsorption (OH$_{ads}$) [5,14–16], surface roughening [17] and H$_2$O$_2$ decomposition [18]. In contrast, the commercial carbon supported Pt-M alloy catalyst (*e.g.*, Pt-Co/C) can only improve 2–3 times mass activity over state-of-the-art Pt/C catalysts [4]. It has been well recognized that good alloy structure, homogeneous composition and uniform small particle size are key factors for a highly active Pt-M/C catalyst [3]. A common preparation method to Pt-M alloy catalysts is based on a second deposition route [23,24], namely, depositing M precursor onto a pre-synthesized Pt/C, subsequently followed a high temperature treatment to form Pt-M alloy. However, the heat-treatment process will result in both metal particles agglomeration (reduction in metal surface area) and

\* Corresponding author. Tel.: +1 906 487 2298; fax: +1 906 487 3213.
\*\* Corresponding author. Tel.: +1 951 827 2068; fax: +1 951 827 5696.
 *E-mail addresses:* wzli@mtu.edu (W. Li), Yushan.Yan@ucr.edu (Y. Yan).
 [1] Present address: Department of Chemical Engineering, Michigan Technological University, 1400 Townsend Drive, Houghton, MI 49931, USA.
 [2] Present address: Department of Chemical Engineering, Nanotechnology Institute and Waterloo Institute for Sustainable Energy, University of Waterloo, 200 University Avenue West, Waterloo, Ontario, Canada N2L 3G1.
 [3] Present address: Key Lab for Nanomaterials of Ministry of Education, Beijing University of Chemical Technology, 15 Bei San Huan East Road, Beijing 100029, PR China.

poor metal particles dispersion on the carbon support [23]. Colloid synthesis methods have been emerged as a new approach for preparing Pt-M alloy/C catalysts, and these methods focus on synthesis of metal nanoparticles colloidal solution, and then deposition of the colloids onto a suitable support material, such as carbon black or activated carbon. Various protective agents [25–27], *e.g.*, polymers, surfactants, ligands, interacting with the Pt and Pt-M surfaces, have been used to stabilize the colloids in solvent. Generally, a heat-treatment is required to remove these stabilizers. A simple polyol synthesis approach has recently attracted enormous attention [18,28–36]. The nanoparticles of metals or their alloys, such as Pt [28–31], Pt-Ru [32,33], Pt-Fe [18], Pt-Pd [34], Pt-Sn [32,35,36], etc., were reduced in an ethylene glycol (EG) solvent without presence of any stabilizers. The size of noble metal/metal alloy nanoparticles can be easily controlled by adjusting the synthesis conditions, such as pH or EG concentration. The EG method offers a big advantage that EG can be easily washed away by DI water. However, this method was not successful, when it was applied to preparation of noble metal–base metal alloy catalysts, such as Pt-Fe/C catalyst [18]. The main issue is that less Fe deposition (only 1/3–1/5) in the final catalyst as compared with the initial Fe amount in the precursor, and this is mainly due to the weak reducing ability of EG and comparatively low reduction temperature (130–140 °C). In addition, Pt-Fe can hardly form an alloy structure, probably because of the lack of initially intimate contact between the two types of metals (noble metal Pt and base metal Fe) with incompatible natures, and large redox potential gap between them.

Recently, an elegant solution-phase synthesis approach to self-organized FePt magnetic nanoparticles with controlled assembly thickness and surface roughness was successfully developed by the IBM researchers [37,38]. Sun et al. prepared a 3-D array of 4 nm Fe-Pt nanoparticles with a superior magnetic property [38]. Later, the nanoparticles with special structures, such as Pt-Fe cube [39,40], Fe-Pt@Fe$_3$O$_4$ core–shell [41], were also prepared *via* modified synthesis routes. Some attempts to prepare carbon supported Pt-M catalysts (Pt, Pt-Ru, Pt-V-Fe, etc.) using similar synthesis route [42–45], however, encounter a problem in removing the organic protective agents, that is a heat-treatment process at 450–550 °C is normally required to remove these stabilizers, and this process results in Pt-M nanoparticles agglomeration and poor distribution on the carbon support, eventually limits their electrocatalytic mass activity enhancement.

In the present paper, we modified this novel solution-phase synthesis method to electro-catalyst preparation. Ultra-fine Pt-Co nanoparticles with controlled composition and homogeneous dispersion on the carbon support (carbon black and carbon nanotubes) were successfully prepared. The composition of Pt-Co/C catalyst was analyzed by inductively coupled plasma atomic emission spectroscopy (ICP-AES) and energy dispersive X-ray spectroscopy (EDS), the particle size and alloy structure of Pt-Co bimetallic nanoparticles were characterized by X-ray diffraction (XRD) and transmission electron microscopy (TEM). The ORR catalytic activity of the Pt-Co/C was directly evaluated in a single PEM fuel cell configuration, with comparison to commercial Pt/C catalyst.
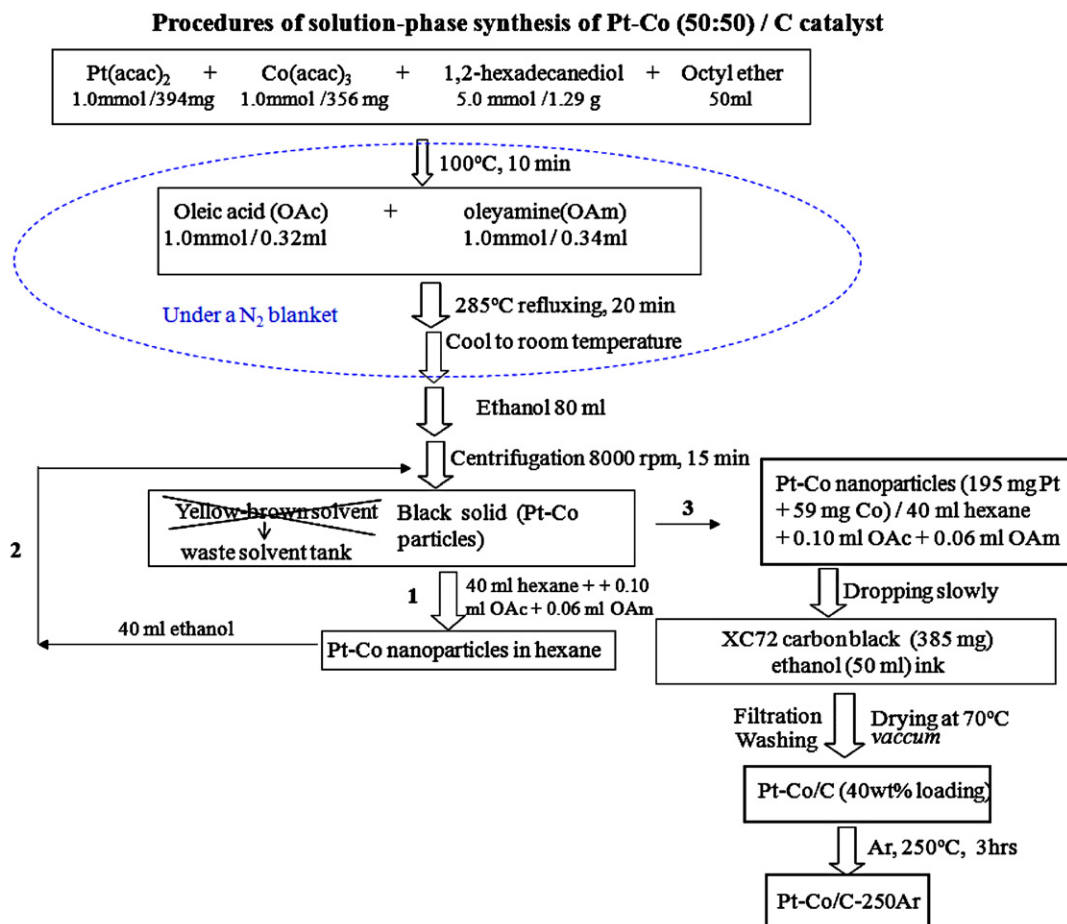


**Fig. 1.** Procedures of the solution-phase synthesis method for preparing Pt-Co/C (40 wt%) catalyst.

## 2. Experimental

### 2.1. Catalyst preparation

The detailed procedures of preparation of Pt-Co/C catalysts are shown in Fig. 1, which include synthesis of Pt-Co nanoparticles and deposition of Pt-Co nanoparticles onto C supports.

#### 2.1.1. Synthesis of Pt-Co nanoparticles

The solution-phase synthesis of Pt-Co nanoparticles is based on a reported IBM method [38] with minor modifications, and can be described as follows: Pt(acac)$_2$ (394 mg, 1.0 mmol), Co(acac)$_3$ (356 mg, 1.0 mmol), 1,2-hexadecanediol (1.29 g, 5.0 mmol), and octyl ether (50 ml) were added into a flask equipped with a N$_2$ in/outlet, refluxing tube, and a thermal couple. The mixture was heated by a mantle to 100 °C under a blanket of N$_2$ for 10 min, during this period, oleic acid (OAc, 0.32 ml, 1.0 mmol) and oleylamine (OAm, 0.34 ml, 1.0 mmol) were added, and then the mixture was heated to reflux at 285 °C for 20 min to reduce Pt$^{2+}$ and Co$^{3+}$ and form Pt-Co alloy. The heating was then stopped and the mantle heater was removed as the temperature decreased to 200 °C, the black reaction mixture was subsequently cooled down to room temperature. After ethanol (80 ml) was added under ambient condition, the black solid was precipitated and separated by centrifugation (8000 rpm, 15 min). The yellow-brown supernatant was discarded and the black precipitation was dispersed in hexane (40 ml) in the presence of OAc (0.10 ml) and OAm (0.06 ml). The black colloid was then precipitated out by adding ethanol (40 ml) and separated with centrifugation (8000 rpm, 15 min) three times for sample cleaning. The product, Pt$_{50}$Co$_{50}$ nanoparticles (molar ratio of 50:50, denoted as Pt-Co), was finally redispersed in hexane solvent in the presence of OAc and OAm for preparation of Pt-Co/C catalyst later.

For preparing PtCo nanoparticles, 25 ml ethanol was added to 16 ml hexane containing PtCo nanoparticle colloid to get the precipitation, which was filtered and washed by copious ethanol and water, subsequently dried at 70 °C in *vacuum*. In order to investigate the effects of reduction conditions for Co, (1) we used Co(acac)$_2$ to replace Co(acac)$_3$ as precursor; (2) we injected a strong reducing agent LiBet$_3$H into the synthesis system at 200 °C, to prepare Pt-Co nanoparticles, and denoted as Pt-Co(2+) and Pt-Co(Li), respectively. Pt-Fe nanoparticles were also prepared according to same processes as above mentioned, with Fe(acac)$_2$ as precursor. The Pt-M atomic ratios in all Pt-M samples were kept at 50:50.

### 2.2. Preparation of Pt-Co/C catalysts

The catalyst support was commercial Vulcan XC-72 carbon black (Carbot Corp.) without further treatment. 50 ml ethanol was mixed with 385 mg carbon black and then was ultrasonically agitated for 10 min to prepare carbon ink. 40 ml hexane solution with 195 mg Pt and 59 mg Co (based on calculation from their precursors) was slowly added to the carbon ethanol ink under vigorous stirring. The Pt-Co/C (*as prepared*) catalyst with metal loading of 40 wt% was finally obtained after filtrating, washing (>1 L ethanol and >1 L DDI water) and drying in *vacuum* at 70 °C (catalyst preparation procedures are listed in Fig. 1). The filtrate is pure and colorless, which indicates a full deposition of Pt-Co nanoparticles onto carbon support. The *as prepared* Pt-Co/C catalyst was heat-treated under Ar atmosphere at 250 °C for 3 h to remove organic surfactants (OAc and OAm) and to clean the catalyst surface. The finish sample was denoted as Pt-Co/C-250Ar (40 wt%). We used same quantity of carbon ink and reduced the volume of hexane containing Pt-Co nanoparticles by half to prepare Pt-Co/C catalyst with a metal loading of 20 wt%. Multi-walled carbon nanotube (MWNT, diameter: 30–50 nm, MER Corp.) was also used as support to prepare

20 wt% Pt-Co/MWNT. Pt-Co(2+), Pt-Co(Li) and Pt-Fe nanoparticles were deposited onto carbon support according to a similar synthesis route as above mentioned and denoted as Pt-Co/C(2+), Pt-Co/C(Li) and Pt-Fe/C. No heat-treatment process performed on these samples and the Pt-M metal loading was maintained at 40 wt%.

### 2.3. Catalyst characterization

Thermogravimetric analysis was carried out on a high resolution TGA instrument (Mettler/Toledo, SDA851e). A 5.5 mg of Pt-Co nanoprticle or Pt-Co/C was put into the sample holder and then the test chamber was heated from room temperature to 800 °C at a heating rate of 5 °C min$^{-1}$ under air. TGA data was recorded and analyzed by a linked computer using STARe software V.1.0.

ICP-AES and EDS were conducted to determine the Pt and Co element ratios in the Pt-Co/C catalysts. For ICP-AES, the Pt-Co/C catalysts were dissolved in an aqua regia solution ('royal water'), and then diluted to prepare solution with 3–10 ppm Pt$^{2+}$ or Co$^{3+}$. Element analyses of Pt$^{2+}$ and Co$^{3+}$ concentrations in the solutions were performed on an ICP-AES instrument (PerkinElmer, Optima3000DV). A PHILIPS XL30-FEG SEM instrument was used to perform EDS, a small amount of catalyst powder was pasted on the holder surface using a small piece of conducting tape, and then was put into the SEM chamber, five spots with around 20 × 20 μm$^2$ were detected for each sample and the average Pt-Co element ratio was reported.

Transmission electron microscopy (TEM) characterizations were carried out on a Philips CM300 instrument operating at 120 kV. Samples for TEM analysis prepared by drying catalyst ethanol inks on amorphous carbon coated copper grids, particle size distribution were determined by counting more than 300 particles.

Powder XRD patterns were obtained on a Brucker X-ray diffraction meter using Cu-Kα radiation with a Ni filter. The tube current is 40 mA and tube voltage is 40 kV. The 2θ angular regions between 20° and 85° were explored at a scan rate of 5° min$^{-1}$ with an angular resolution of 0.02°. The mean Pt-Co particle size was calculated from Debye–Scherrer formula based on the Pt(2 2 0) diffraction peak.

### 2.4. Membrane electrode assembly (MEA) fabrication and PEMFC test

Four MEAs consisting of cathode with Pt-Co/C and commercial Pt/C (as reference) were prepared. The polymer electrolyte for the MEA is a treated Nafion membrane 112 or 115, and the treatment procedures can be found somewhere else [46]. Pt/C (20 wt%, E-TEK) and Pt-Co/C (20 wt%, 250Ar) mixing with 5 wt% Nafion solution (dry Nafion weight ratio is 30 wt%) were brushed directly on a gas diffusion layer (GDL, 25CC, SGL Corp.) to prepare the anode and cathode, respectively. The catalyst loading was maintained at 0.2 mg Pt cm$^{-2}_{\text{electrode}}$. The MEA with an active electrode area of 4.41 cm$^2$ (2.1 cm × 2.1 cm) were obtained by hot-pressing a cathode, a treated Nafion 112 or 115 membrane (3 cm × 3 cm) and an anode with a pressure of 50 kg cm$^{-2}$, at 135 °C for 1.5 min. The reference MEA was obtained by hot-pressing two Pt/C based electrodes according to same experimental conditions mentioned above. The PEMFC performances for the four MEAs were tested in an Arbin fuel cell test stand. The operation conditions are as follows: the oxygen and hydrogen operation pressures were 35 psi and their flow rates were 200 ml min$^{-1}$, the temperature of cell, anode and cathode humidifier was 70, 75 and 75 °C, respectively. The polarization *I–V* curves were collected after 2 h activation at constant operation voltage of 0.6 V.

## 3. Results and discussion

Using Pt-Co/C (40 wt%) as an example, the procedures of synthesis of Pt-M/C catalyst *via* the solution-phase reduction method are illustrated in Fig. 1. The heating of Co(acac)$_3$ and Pt(acac)$_2$ mixture in the presence of oleic acid (OAc), oleylamine (OAm), and 1,2-hexadecanediol refluxing at 285 °C leads to monodisperse 2–3 nm Pt-Co nanoparticles. A hexane solvent containing the fine Pt-Co nanoparticle colloid was then slowly dropped into carbon black ethanol ink to form homogeneously dispersed Pt-Co/C catalyst. Since the stabilizers (OAc and OAm) tend to aggregate in polar solvent ethanol, thus leaving Pt-Co nanoparticles depositing onto carbon support. Finally, an optimized temperature of 250 °C was used for 3 h to remove organic stabilizers, while maintain small PtCo nanoparticles (<3 nm).

TGA was conducted to determine the Pt-Co metal loading as well as analyze the amount of residues (organic protective agents, etc) left in the catalyst, as shown in Fig. 2. The blue dot line represents the weight loss percentage of Pt-Co nanoparticle after copious ethanol washing. It is observed *ca.* 12% weight loss from 100 to 250 °C, which can be mainly attributed to the loss of organic stabilizers of OAc and OAm. It was reported that around 50 wt% OAc and OAm covered the catalyst surface without the ethanol washing process [44], using same molar ratio of metals to stabilizers (1:1). In our case, copious ethanol washing is believed to account for the removal of majority of organic stabilizers. The solid black and red lines are the weight loss percentage for Pt-Co/C and Pt-Co/C-250Ar (heat-treatment at 250 °C for 3 h) catalysts. It is interesting to observe that the weight loss of Pt-Co/C-250Ar sample is very low (<4%), which indicates most organic stabilizers (OAc and OAm) can be removed at a moderate temperature of 250 °C. This is an appropriate temperature for heat-treatment of the Pt-Co/C catalysts. Further TEM characterizations show that Pt-Co nanoparticles do not undergo observable agglomeration after the heat-treatment of 250 °C under inert gas. Luo et al., reported that some organic compounds, such as decanethiol or oleylamine, were employed to stabilize the nanoparticles by interacting with the Au-Pt or Pt-V-Fe nanoparticles surface, however, high temperature (*e.g.* 500 °C) is usually required to remove the stabilizers as well as to clean the catalyst surface and enhance catalyst electric conductivity [42–46]. In our case, the Pt-Co/C catalysts were treated under an inert gas atmosphere at a comparatively low temperature, which was sufficient to remove majority of organic stabilizers. The TGA curves also show around 42 wt% metal or metal oxide left after heating-treatment, which is slightly higher than the setting loading of
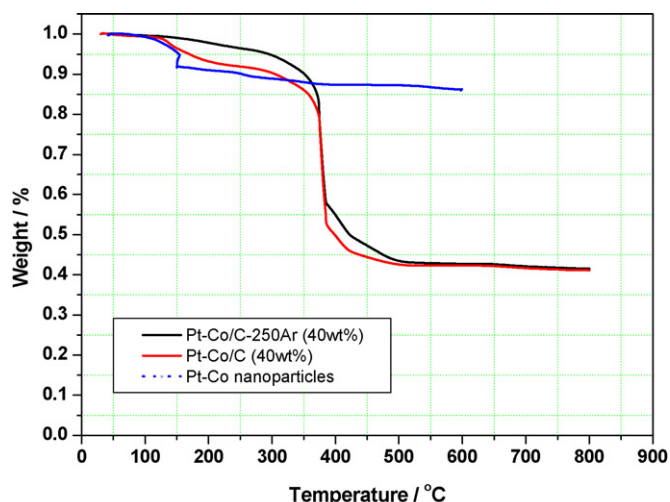
**Table 1**
Element compositions of Pt-Co/C catalysts determined by SEM-EDS and ICP-AES.

| | Pt-Co (ICP-AES) | Pt-Co (SEM-EDS) |
|---|---|---|
| Pt-Co/C | 58:42 | 57:43 |
| Pt-Co/C (2+) | 56:44 | 55:45 |
| Pt-Co/C(Li) | 49:51 | 50:50 |

40 wt%. Considering Co could be oxidized to Co$_2$O$_3$/Co$_3$O$_4$ at a high temperature and increase the sample weight, this method offers a convenient way to accurately control Pt-Co metal loading just by altering the ratio of dispersed Pt-Co nanoparticles to the carbon support in the catalyst synthesis process.

The element ratios of Pt and Co in the Pt-Co/C catalysts were measured by both ICP-AES and EDS, as shown in Table 1. The Pt-Co ratio of Pt-Co/C is 57:43 (EDS) and 58:42 (ICP-AES). As we know, ICP-AES gives bulk elements composition of a material, while SEM-EDS provides surface elements composition in a small portion of the material (*e.g.*, $20 \times 20 \, \mu m^2$). The Pt-Co ratios obtained from SEM-EDS are the average results through detecting five different areas for each sample, since the element ratios from ICP-AES and EDS are very close, this indicates these Pt-Co/C catalysts have uniformly mixing of Pt and Co metals. We used Co(acac)$_2$ (Co2$^+$) as precursor to prepare Pt-Co/C(2+) catalyst, and found it has a similar Pt-Co ratio (EDS: 55:45; ICP-AES: 56:44) as Pt-Co/C (Co$^{3+}$ as precursor). However, the Pt-Co ratios in catalysts are higher than the initial precursor Pt-Co ratio of 50:50 for both Pt-Co/C samples prepared using different Co precursors (Co$^{3+}$ and Co$^{2+}$), this indicates that 1-2-hexanedecandiol, even at over-stoichiometric amount (reducing agent: precursor = 2.5:1), cannot fully reduce Co$^{3+}$/Co$^{2+}$ to Co at the given synthesis conditions (285 °C for 20 min). 15% Co for Pt-Co/C(3+) and 10% Co for Pt-Co/C (2+) cannot be reduced and deposited onto the carbon support. In comparison, the Pt-Co/C-Li prepared by an injection of LiBEt$_3$H has a Pt-Co ratio of 49:51 (ICP), which is very close to the setting ratio of 50:50. This means the strong reducing agent LiBEt$_3$H can fully reduce Co$^{3+}$/Co$^{2+}$ to Co.

Typical TEM images of Pt-Co/C samples with different metal loadings and with/without heat-treatment are shown in Fig. 3. Small spherical Pt-Co nanoparticles are homogeneously dispersed on carbon black and have narrow size distribution, ranging from 2 to 4 nm, for both 20 and 40 wt% samples (see Fig. 3a and c). In addition, nearly no observable metal nanoparticles agglomerations were found after the heat-treatment at 250 °C under Ar atmosphere, shown in Fig. 3b and d. The TEM image of Pt-Co/C (2+) shows Pt-Co nanoparticles are as small as 2–3 nm and deposited uniformly on carbon support, which is just like Pt-Co/C (Fig. 3e). However, Pt-Co/C (Li) prepared by additional injection of LiBEt$_3$H has some particle aggregates (Fig. 3f), though the average particle size can be controlled <3 nm. We also used this solution-phase synthesis method to prepare MWNT supported Pt-Co and carbon black supported Pt-Fe catalysts. It is interesting to observe that both Pt-Co/MWNTs and Pt-Fe/C have very small particle size, uniform particle size distribution (2–4 nm) and homogeneous particles dispersion on the carbon supports (see Fig. 3g and h). This suggests that this solution-phase reduction route is an effective approach to prepare a broad spectrum of fine noble metal–cheap metal alloy nanoparticles supported on different carbon materials.

Fig. 4 shows the powder XRD patterns of carbon supported Pt-Co catalysts with different loadings and with/without heat-treatment. The diffraction peaks of the face centered cubic (fcc) Pt lattice – Pt(1 1 1), Pt(2 0 0), Pt(2 2 0), Pt(3 1 1) are clearly recognizable in all XRD patterns. It is known that the diffraction peaks become broader as the particle size gets smaller, based on Debye–Scherrer formula. Possible influence of the support on the lattice structure of these nano-sized Pt-Co/C catalysts are not accounted for the lattice parameter calculation, however, such influences are expected
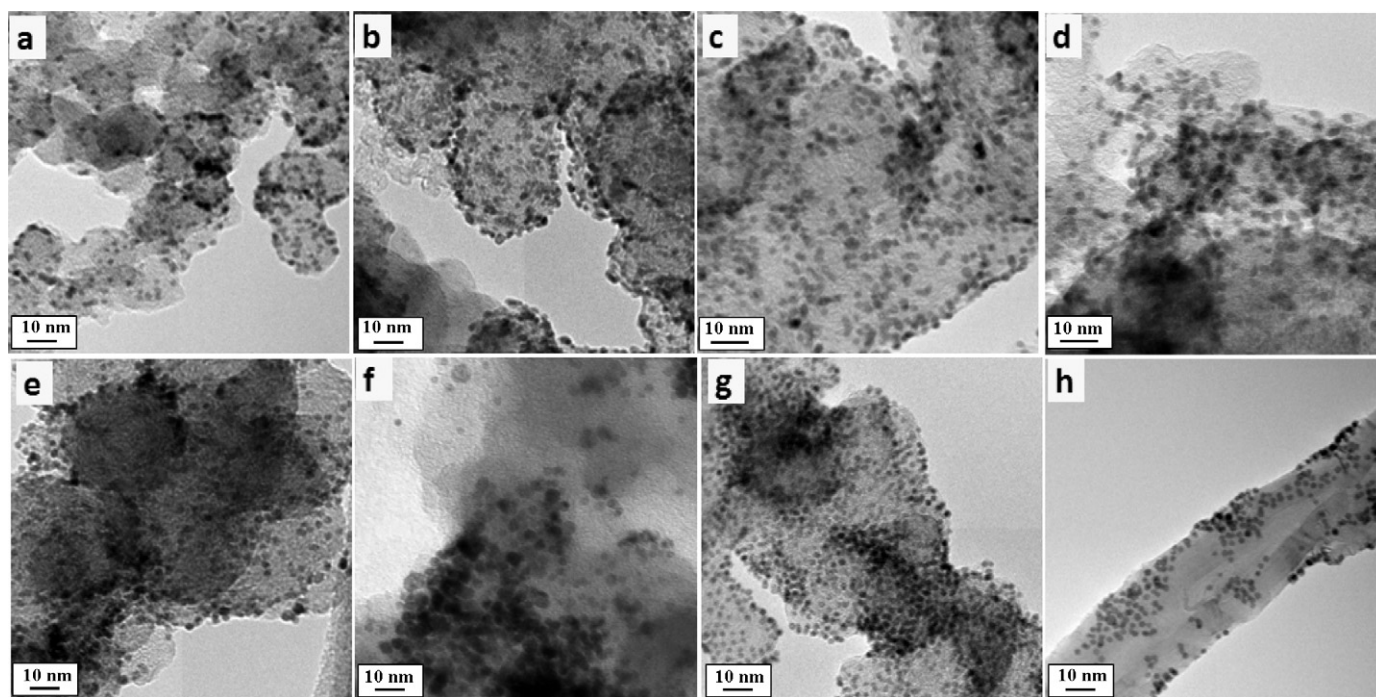


**Fig. 2.** TGA curves of Pt-Co/C, Pt-Co/C-250Ar catalysts and Pt-Co nanparticles.

**Fig. 3.** TEM images of (a) Pt-Co/C (20 wt%), (b) Pt-Co/C-250Ar (20 wt%), (c) Pt-Co/C (40 wt%), (d) Pt-Co/C-250Ar (40 wt%), (e) Pt-Co/C(2+) (40 wt%), (f) Pt-Co/C(Li) (40 wt%), (g) Pt-Fe/C (40 wt%), and (h) Pt-Co/MWNT (20 wt%) catalysts.

to be small for the system studied here. Particle size and lattice parameters for these Pt-M/C catalysts are shown in Fig. 4. The mean particle size of Pt-Co/C-250Ar (40 wt%) catalyst is around 2.3 nm, which is slightly larger than that of Pt-Co/C sample (<2.0 nm). This is in good agreement with the TEM images. The absence of diffraction peaks typical for Co, $Co_2O_3$ and $Co_3O_4$ can be attributed to reasons such as Co being dissolved in Pt lattice, that is, forming a Pt-Co alloy, and/or Co being in present in the amorphous form. The position of the Pt(1 1 1) peak for all Pt-Co/C samples is shifted to a higher 2-theta-position (40.69°) than that for pure Pt, whose maximum diffraction peak Pt(1 1 1) is at 39.76°. The lattice parameter of pure Pt fcc phase is 3.920 Å, while those of the heat-treated Pt-Co/C-250Ar catalysts are 3.872 Å (20 wt%) and 3.868 Å (40 wt%).

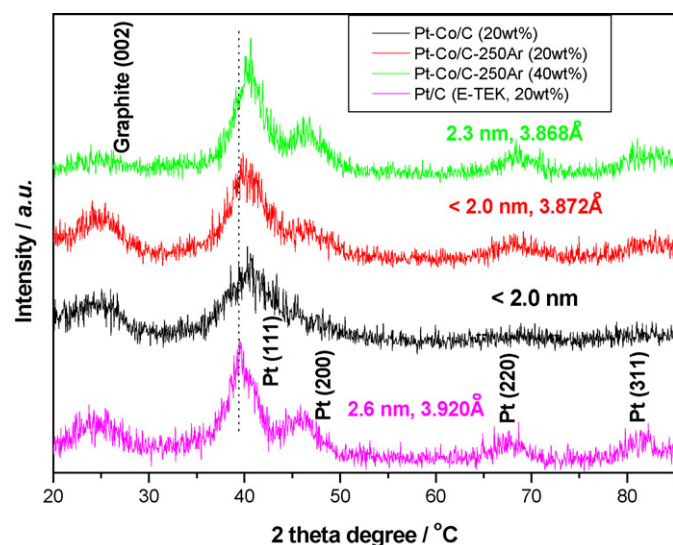This indicates good Pt-Co alloy has been formed even treated at a moderate temperature of 250 °C. Therefore, we believe that in this high boiling point organic phase reduction system, an intimate Pt-Co precursors interaction and a reduced redox potential difference in organic medium between Pt and Co might result in a good mixture of Pt and Co crystal seeds, thus leading to a small particle size and an excellent Pt-Co initial contact, which will benefit the formation of Pt-Co alloy at moderate temperature treatment. Further, it should be noted that with the heat-treatment temperature of 250 °C, the Pt-Co/C catalyst does not show any supper lattice CoPt fct crystalline diffraction peaks, *e.g.* CoPt(1 1 0) or CoPt(2 1 0).

Since PEMFC performance is an ultimate electrocatalytic activity test for Pt-Co/C, we directly investigated the polarization curve of single PEMFC employing the Pt-Co alloy/C as cathode catalyst, as shown in Fig. 5a. Two types of Nafion membranes (112 and 115) were used as PEMFC electrolyte, the Nafion 112 based MEAs exhibit better PEMFC performances than the Nafion 115 based ones. This clearly shows that thinner electrolyte membrane can effectively reduce cell inner resistance and improve mass transport. The Pt-Co/C-250Ar based MEAs show better fuel cell performances at low (<0.2 A cm$^{-2}$) and medium (0.2–1.5 A cm$^{-2}$ for Nafion 112 based MEAs, 0.2–0.7 A cm$^{-2}$ for Nafion 115 based MEAs) current density regions. As shown in Fig. 5b, at operation voltage of 0.9 V, the Pt-Co/C-250Ar based MEA has a mass activity of 0.30 A mg$_{Pt}^{-1}$, which is 2.3 times higher than that of Pt/C based MEA (0.13 A mg$_{Pt}^{-1}$). In Fig. 5b, we compared the benchmark activity of Pt/C and Pt-Co/C catalysts with self-made Pt-Co/C-250Ar catalyst [4], although the mass activity of Pt/C in this study is lower than the benchmark activity (0.13 vs. 0.16 A mg$_{Pt}^{-1}$), self-prepared Pt-Co/C-250Ar shows slightly higher mass activity than the benchmark for commercial Pt-Co/C catalyst (0.30 vs. 0.28 A mg$_{Pt}^{-1}$). At an operation voltage of 0.8 V, the PtCo/C based MEA (with Nation 112 membrane) can reach a power density of 320 mW cm$^{-2}$, while the Pt/C based MEA's power density is 240 mW cm$^{-2}$. For a fuel cell electrocatalyst, mass activity = electrochemical sur-



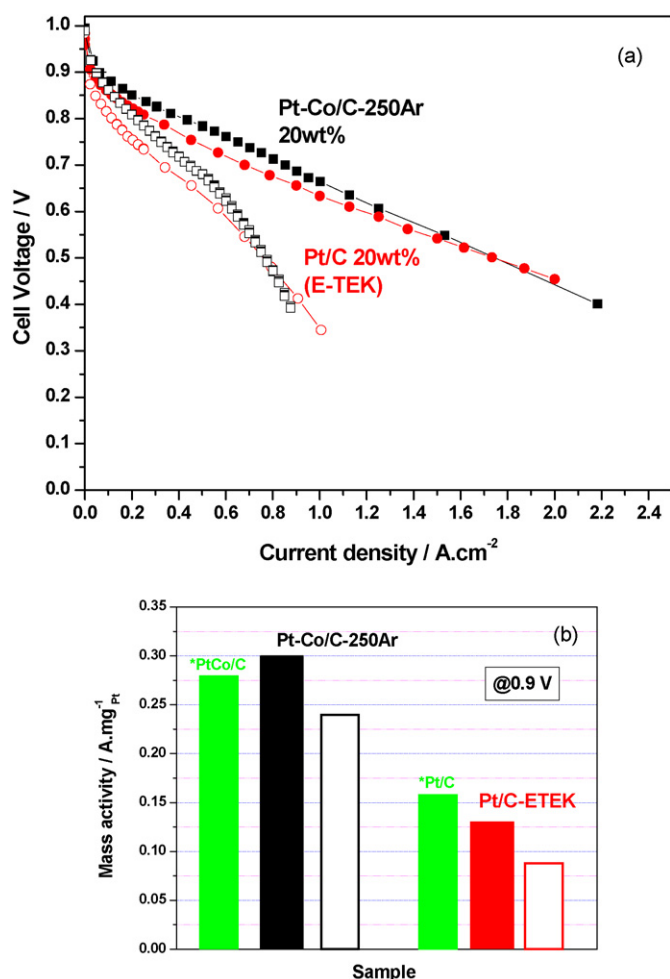**Fig. 4.** Powder XRD patterns of Pt/C (20 wt%, E-TEK) and Pt-Co/C catalysts.

**Fig. 5.** (a) Polarization curves of PEMFCs with Pt/C (red line) and Pt-Co/C-250Ar (black line) cathode catalysts, (b) mass activity at 0.9 V for commercial Pt/C (E-TEK) and Pt-Co/C-250Ar cathode catalysts. Anode: Pt/C (E-TEK, 20 wt%), 0.2 mgPt cm$^{-2}$, cathode: 0.2 mgPt cm$^{-2}$. Electrolyte: solid: Nafion 112; hollow: Nafion 115. Test conditions: cell: 70 °C, 100% RH, Anode and cathode: H$_2$ and O$_2$; flow rate: 0.2 L min$^{-1}$, backpressure: 35 psi. (*) The green columns in (b) represent the benchmark mass activity of Pt/C (46 wt%, TKK) and Pt-Co/C (TKK) in Nafion 112 based MEAs under standard PEMFC tests [4]. (For interpretation of the references to color in this figure legend, the reader is referred to the web version of the article.).

## 4. Conclusions

In this paper, we reported a solution-phase synthesis method for preparing carbon (carbon black and carbon nanotubes) supported Pt-M (Pt-Co and Pt-Fe) alloy catalysts. The Pt and M organic precursors (Pt(acac)$_2$, Co(acac)$_3$, Co(acac)$_2$, Fe(acac)$_2$) were used as metal precursors, which were reduced in a high boiling point solvent octyl ether in the presence of oleic acid and oleylamine as stabilizers to synthesize Pt-Co/Pt-Fe alloy nanoparticles. The TGA indicates that the stabilizers can be removed through copious ethanol washing and moderate temperature heat-treatment (250 °C) under an inert gas atmosphere (Ar). TEM images show the *as prepared* Pt-M/C catalysts have very small nanoparticles homogeneously dispersed on the carbon support (carbon black and CNTs), with a particle size distribution of 2–4 nm. The Pt-Co nanoparticles do not aggregate observably after 3-h-heat-treatment under Ar. XRD analyses further indicate the average particle size remains around 2.3 nm, and the lattice parameter is 3.868 Å for Pt-Co/C-250Ar. The element analysis techniques of ICP-AES and SEM-EDS show that the Pt-Co ratio of final nanoparticles is slightly higher than the initial Pt-Co ratio in their precursors, which suggests little amount of Co cannot be fully reduced and deposited on carbon support. Addition of small amount of strong reducing agent LiBEt$_3$H can help to fully reduce and deposit Co, however, results in Pt-Co particles agglomeration. PEMFC tests on the MEAs (with Nafion 112 membrane) show that the mass activity of Pt-Co/C is 0.30 A mg$_{Pt}^{-1}$, which is 2.3 times higher than that of Pt/C (0.13 A mg$_{Pt}^{-1}$) at a working voltage of 0.9 V, this can be attributed to its smaller particle size and superior lattice parameter. This solution-phase synthesis approach is very promising for preparing other highly active carbon supported Pt-M nanocatalysts, such as Pt-Ni/C, Pt-Ru/C, and Pt-Ni@Pt core shell/C, etc.

## References

[1] W. Vielstich, A. Lamm, H. Gasteiger, Handbook of Fuel Cells, John Wieley & Sons Inc., 2004.
[2] E. Yeager, Electrocatalysts for oxygen reduction, Electrochim. Acta 29 (1984) 1527–1537.
[3] T.R. Ralph, M.P. Hogarth, Platinum Met. Rev. 46 (2002) 3–14.
[4] H.A. Gasteiger, S.S. Kocha, B. Sompalli, F.T. Wagner, Appl. Catal. B. Environ. 56 (2005) 9–35.
[5] V. Stamenkovic, B. Fowler, B.S. Mun, G.F. Wang, P.N. Ross, C.A. Lucas, N.M. Markovic, Science 315 (2007) 493–497.
[6] J.K. Norskov, J. Rossmeisl, A. Logadottir, L. Lindqvist, T. Bligaard, H. Jonsson, J. Phys. Chem. B 46 (2004) 17886–17892.
[7] K. Kinoshita, Electrochemical Oxygen Technology, John Wiley & Sons Inc, New York, 1992.
[8] P.N. Ross, Handbook of Fuel Cells, Vol. 2 Electrocatalysis, John Wieley & Sons Inc., 2004, p. 465.
[9] V. Jalan, J. Electrochem. Soc. 129 (1982) C115–115.
[10] V. Jalan, E.J. Taylor, J. Electrochem. Soc. 130 (1983) 2299–2301.
[11] S. Mukerjee, S. Srinivasan, M.P. Soriaga, J. Mcbreen, J. Electrochem. Soc. 142 (1995) 1409–1422.
[12] T. Toda, H. Igarashi, H. Uchida, M. Watanabe, J. Electrochem. Soc. 146 (1999) 3750–3756.
[13] T. Toda, H. Igarashi, M. Watanabe, J. Electroanal. Chem. 460 (1999) 258–262.
[14] V. Stamenkovic, T.J. Schmidt, P.N. Ross, N.M. Markovic, J. Phys. Chem. B 106 (2002) 11970–11979.
[15] V. Climent, N.M. Markovic, P.N. Ross, J. Phys. Chem. B 104 (2000) 3116–3120.
[16] N.M. Markovic, H.A. Gasteiger, P.N. Ross, J. Phys. Chem. B 100 (1996) 6715–6721.
[17] M.T. Paffett, J.G. Beery, S. Gottefeld, J. Electrochem. Soc. 135 (1988) 1431.
[18] W. Li, W. Zhou, Z. Zhou, H. Li, Z. Zhou, B. Zhou, G. Sun, Q. Xin, Electrochim. Acta 49 (2004) 1045–1055.
[19] S.R. Brankovic, X. Wang, R.R. Adzic, Surf. Sci. 474 (2001) 173–179.

face are (ECSA) × specific activity, smaller particle size will give higher ECSA. The reduced Pt-Pt neighboring distance will favor the bridge adsorption of oxygen, and facilitate cleavage of the O=O bond [4,10], thus improving the ORR specific activity. Therefore, the improved mass activity for Pt-Co/C can be reasonably attributed to (1) its smaller particle size (<2.0 nm *vs.* 2.6 nm), and (2) reduced lattice parameter (3.872 Å *vs.* 3.920 Å). However, at high current density region (>1.5 and 0.7 A cm$^{-2}$ for Nation 112 and 115 based MEAs, respectively), the two Pt-Co/C-250Ar based MEAs are slightly lower than the corresponding commercial Pt/C based MEAs, this is probably attributed to the impurities of Pt-Co/C catalyst surface (surrounded by trace organic stabilizers), thus impeding the mass transport of reactants. More characterizations and analysis are needed to investigate the mass transport issue, further optimization of the catalyst layer structure for the self-made Pt-Co/C based MEA is expected to improve the PEMFC performance at high current density region. This solution-phase method is promising to prepare other Pt based bi-, tri-metallic catalysts, *e.g.* carbon supported Pt-Ni, Pt-Ru, and Pt-Ni@Pt core shell nanostructures, these work are currently under way in our groups.

[20] J.L. Zhang, M.B. Vukmirovic, Y. Xu, M. Mavrikakis, R.R. Adzic, Angew. Chem. In. Ed. 4 (2005) 2132–2135.
[21] J.L. Zhang, K. Sasaki, E. Sutter, R.R. Adzic, Science 315 (2007) 220–222.
[22] S. Koh, P. Strasser, J. Am. Chem. Soc. 129 (2007) 12624–12625.
[23] M.K. Min, J.H. Cho, K.W. Cho, H. Kim, Electrochim. Acta 45 (2000) 4211–4217.
[24] K. Hiroshima, T. Noritake, Y. Ohya, Y. Marimoto, Fuel cells 2 (2002) 31–35.
[25] N. Toshima, T. Yonezawa, New J. Chem. 22 (1998) 1179–1201.
[26] H. Bonnemann, R.M. Richards, Eur. J. Inorg. Chem. 10 (2001) 2455–2480.
[27] X. Wang, I.M. Hsing, Electrochim. Acta 47 (2002) 2981–2987.
[28] Y. Wang, J.W. Ren, K. Deng, L.L. Gui, Y.Q. Tang, Chem. Mater. 12 (2002) 1622–1627.
[29] W. Li, C. Liang, W. Zhou, J. Qiu, Z. Zhou, G. Sun, Q. Xin, J. Phys. Chem. B 107 (2003) 6292–6299.
[30] Z. Zhou, S. Wang, W. Zhou, G. Wang, L. Jiang, W. Li, S. Song, J. Liu, G. Sun, Q. Xin, Chem. Commun. 3 (2003) 394–395.
[31] Z. Liu, X.H. Lin, J.Y. Lee, W. Zhang, M. Han, L. Gan, Langmuir 18 (2002) 4054–4060.
[32] W. Zhou, Z. Zhou, S. Song, W. Li, G. Sun, P. Tsiakaras, Q. Xin, Appl. Catal. B, Environ. 46 (2003) 273–285.
[33] W. Li, X. Wang, Z. Chen, M. Waje, Y. Yan, J. Phys. Chem. B 110 (2006) 15353–15358.
[34] H. Li, Q. Xin, W. Li, Z. Zhou, L. Jiang, S. Yang, G. Sun, Chem. Commun. 23 (2003) 2776–2777.
[35] W. Zhou, W. Li, S. Song, Z. Zhou, L. Jiang, G. Sun, Q. Xin, K. Poulianitis, S. Kontou, P.P. Tsiakaras, J. Power Sources 131 (2004) 217–223.
[36] L. Jiang, Z. Zhou, W. Li, W. Zhou, S. Song, H. Li, G. Sun, Q. Xin, Energy Fuel 18 (2004) 866–871.
[37] S.H. Sun, G.B. Murray, D. Weller, L. Folks, A. Moser, Science 287 (2000) 1989–1992.
[38] S.H. Sun, S. Anders, T. Thomson, J.E.E. Baglin, M.F. Toney, H.F. Hamann, C.B. Murray, B.D. Terris, J. Phys. Chem. B 107 (2003) 5419–5425.
[39] H. Zeng, P.M. Rice, S.X. Wang, S.H. Sun, J. Am. Chem. Soc. 126 (2004) 11458–11459.
[40] M. Chen, J. Kim, J.P. Liu, H.Y. Fan, S.H. Sun, J. Am. Chem. Soc. 128 (2006) 7132–7133.
[41] H. Zeng, J. Li, Z.L. Wang, L.P. Liu, S.H. Sun, Nano Lett. 4 (2004) 187–190.
[42] J. Luo, P.N. Njoki, Y. Lin, L.Y. Wang, C.J. Zhong, J. Electrochem. Commun. 8 (2006) 581–587.
[43] J. Luo, L.Y. Wang, D. Mott, P.N. Njoki, N. Kariuki, C.J. Zhong, T. He, J. Mater. Chem. 16 (2006) 1665–1673.
[44] Z.F. Liu, M. Shamsuzzoha, E.T. Ada, W.M. Reichert, D.E. Nikles, J. Power Sources 164 (2007) 472–480.
[45] H. Yano, M. Kataoka, H. Yamashita, H. Uchida, M.M. Watanabe, Langmuir 23 (2007) 6438–6445.
[46] M.S. Wilson, S. Gottesfeld, J. Appl. Electrochem. 22 (1992) 1–7.